RSC Advances

ROYAL SOCIETY OF CHEMISTRY

www.rsc.org/advances

Please do not adjust margins

RSC Advances

ARTICLE

Efficient aqueous hydrodeoxygenation of vanillin over mesoporous carbon nitride-modified Pd nanocatalyst

Hezhan Jiang, Xiaolong Yu, Xiaolun Peng, Haifu Zhang, Renfeng Nie*, Xinhuan Lu, Dan Zhou, Qinghua Xia*

Highly mesoporous carbon nitrides (CN) are synthesized through a simple polymerization reaction, including ethylenediamine (EDA), organic chlorides, with nano SiO_2 as hard-template. The degree of polymerization of as-synthesized CN can easily be controlled by varying the organic chlorides. The CN derived from chloroform exhibits a low degree of polymerization, along with a high specific surface area of 315.9 m^2g^{-1} and pore volume of 0.87 cm^3g^{-1}, in which the mesopore volume proportion reaches as high as 90.9 %. Owing to the rich N groups (15.6 wt %), this basic network with open channels renders homogeneously dispersed Pd coordinated in the mesoporous carbonaceous framework and creates a highly active and stable Pd/CN catalyst for the selective hydrodeoxygenation of vanillin at low pressure (<1 MPa) and temperature (<70 ^oC). The best TOF reaches 295.4 h^{-1}, and the Pd/CN catalyst can be used at least 6 times without obvious loss of its catalytic performance.

Introduction

The selective conversion of biomass has become one of the main ways to obtain chemicals and fuels in relieving the fossil energy and environment crisis.[1] For example, lignin can be broken down to phenolic compounds, such as alkyl-substituted phenols, guaiacols and syringols by various approaches.[2] High oxygen and unsaturated degree, however, make the so-called bio-oil have low energy density, low thermal (20 MJ/kg) and chemical stability (pH 2.5).[3] Hence, bio-oil must be upgraded before it can be used as conventional liquid transportation fuel. Up to date, several approaches, hydrodeoxygenation (HDO),[4] zeolite cracking [5] and aqueous-phase reforming [6] have been developed for the bio-oil upgrading. Comparatively, catalytic HDO has recently drawn unprecedented attention because the upgraded products contain less oxygen, providing them with a higher heating value and rendering them chemically more stable than in their unrefined state.

Various catalysts have been developed for HDO of bio-oil. Among the most prominent classes of catalysts are NiMo-based hydrodesulfurization (HDS) catalysts.[7] Although these catalysts are attractive due to their low price, they often suffer from lower activity and rapid loss of activity. The HDO of bio-oil is also performed over other supported precious metals (i.e., Pt, Pd, Ru) [8-10] and metal alloy (Pd-Fe, [11] etc.). Additionally, the conventional support Al_2O_3 is not stable at HDS conditions in presence of the high amount of water in bio-oil. To overcome this flaws, catalysts supported on SiO_2, [12] carbon, [13] ZrO_2, [10] and zeolites [8] have been explored in recent years. Comparatively, carbons, including activated carbon (AC) and carbon nanotubes (CNTs), etc., are often chosen as candidates because of their high mechanical performance and high surface area. It has been recently shown [4] that CNTs/SiO_2 supported Pd or Ru NPs are able to stabilize the emulsion due to the amphiphilic character (hydrophilic (SiO_2 support) and hydrophobic part (CNTs)) and simultaneously catalyze HDO of bio-oil in organic phase or in aqueous phase. These results indicate that it is possible to control the HDO process with the appropriate catalyst design. Delmon et al. [14] extensively investigated sulfided CoMo and NiMo systems by incorporating potassium and platinum as modifiers and used silica and AC to replace Al_2O_3 as supports, and found that introducing surface oxygen species on AC can generate unique active site-support interactions, resulting in promising reactivity and product selectivity. However, the weak interaction of NPs with AC can lead to aggregation or leaching into water; [9] and the dominated microporous structure increases the diffusion resistance in catalytic reaction, [15] which inevitably reduces the catalytic activity. As a consequence, the chemical or catalytic properties of carbons do not always satisfy the sharply increasing demands of catalysis. Thus, there is a need for the design of highly efficient and recyclable catalysts with environmentally-benign characteristics.

Two-dimensional mesoporous carbon nitride (MCN) has recently received a great attention due to its unique properties, including tunable pore structure, high nitrogen content, great electron mobility and rich basic sites. [16] For example, Vinu et al. [17] successfully reported the preparation of MCN with a uniform pore

Hubei Collaborative Innovation Center for Advanced Organic Chemical Materials, & Ministry-of-Education Key Laboratory for the Synthesis and Application of Organic Functional Molecules, School of Chemistry and Chemical Engineering, Hubei University, Wuhan 430062, P.R. China.
E-mail: refinenie@163.com (N. R. Nie); xiaqh518@aliyun.com (Q. H. Xia); Fax/Tel: +86 27 88662747
Electronic Supplementary Information (ESI) available: [details of any supplementary information available should be included here]. See DOI: 10.1039/x0xx00000x
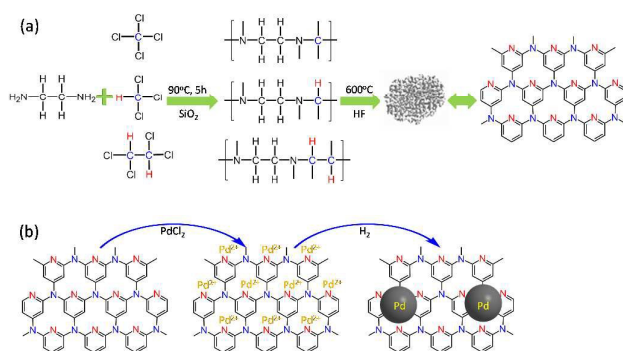
Table 1 Structural properties of the CNs.

Samples	S_{total} (m^2g^{-1})	Pore volume (m^2/g)			V_{meso}/V_{total} (%)	Average pore diameter (nm)
		V_{total} (cm^3/g)	V_{micro} (cm^3/g)	V_{meso} (cm^3/g)		
CN-TE	294.9	0.48	0.07	0.41	84.6	11.2
CN-CF	315.9	0.87	0.08	0.79	90.9	16.6
CN-CT	166.3	0.33	0.06	0.27	81.8	9.2
AC	718.5	0.44	0.24	0.20	45.5	4.3

size distribution using SBA-15 as a template. Groenewolt and Antonietti [18] reported that NPs of graphitic C_3N_4 with different diameters and morphology could be immobilized inside the channels of mesoporous silica host matrices. Many researchers reported that N-doped carbon nanostructures with n-type or metallic behavior have greater electron mobility than their pristine carbon nanostructures. [19] And N-doping can introduce chemically active sites for catalysis and anchoring sites for metal NPs deposition, which is enable the applications of carbon with improved performance in catalysis. [20]

As a model molecule, vanillin (4-hydroxy-3-methoxyben-zaldehyde; a common component of pyrolysis oil) can be effectively hydrogenated into 2-methoxy-4-methylphenol (MMP), which is a potential future biofuel. [9] However, the hydrogenation of vanillin normally requires high hydrogen pressure and high temperature, and always formation of byproduct (4-hydroxymethyl-2-methoxyphenol; HMP) as a result of incomplete hydrogenation due to the low catalytic activity of catalysts. [9, 21, 22] Herein, we synthesize mesopore-dominated CN through a modified polymerization between ethylenediamine (EDA) and organic chlorides using a hard-template route (Scheme 1), and explore its use as a basic host to construct binary Pd/CN heterojunctions for the HDO of vanillin. The influence of the variation of organic chlorides on the textural structure of the carbons, the mophology of Pd NPs and the catalytic performances of Pd/CN are investigated.

Results and discussion

The morphology and structure of as-obtained CNs are surveyed by SEM and TEM images (Fig. S1). SEM images show that CN-CT

displays large particles with less porous and compact structure. In contrast, CN-CF and CN-TE exhibit porous and aerogel-like structure which is constructed by small carbon particles. TEM images show that CN-CF clearly features more abundant inner porosity than that of CN-CT and CN-TE, demonstrating the important role of chloride structure in controlling the morphology of the resultant CNs.

N_2 sorption isotherms strongly support the SEM/TEM results. Steep uptakes at high p/p_0 and clear hysteresis loop presumed to be related to outer surface features and the presence of mesoporous domains (Fig. 1),[17] which are consistent with the corresponding pore size distribution. Compared with CN-CT (166.3 m^2/g, 9.2 nm, Table 1), higher BET areas and pore sizes for CN-CF (315.9 m^2/g, 16.6 nm) and CN-TE (294.9 m^2/g, 11.2 nm) can be observed. Moreover, the CN-CF processes pore volume of 0.87 cm^3/g with a mesopore volume proportion of 90.9 %, much higher than that of CN-CT (0.33 cm^3/g, 81.8 %) and CN-TE (0.48 cm^3/g, 84.6 %). This exclusively originated from the newly-generated void spaces between the particles thanks to the incomplete
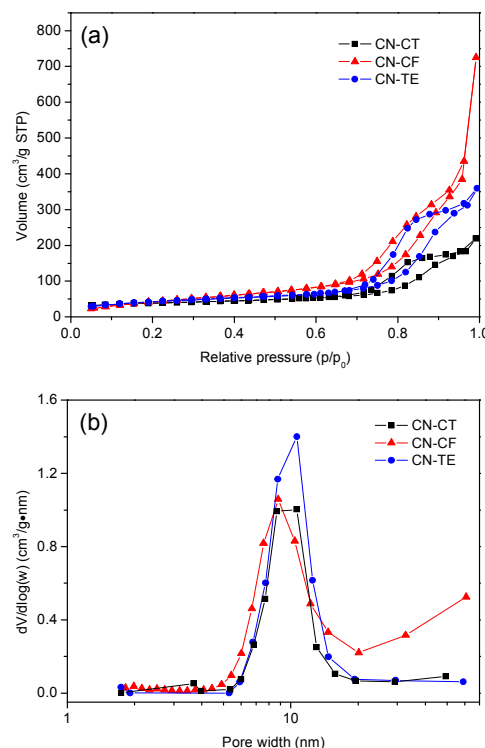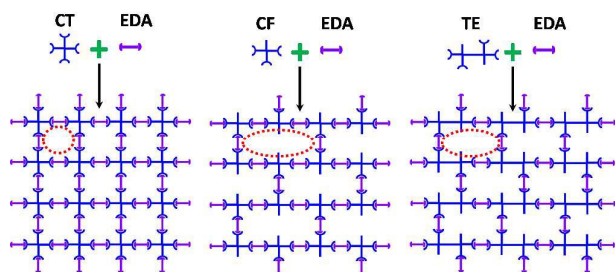

Scheme 1 (a) Synthetic routes to CN, (b) a controllable route to Pd/CN hybrid materials.

Fig. 1 (a) Nitrogen sorption isotherms and (b) pore size distribution of CNs.

Scheme 2 The possible mechanism of EDA and organic chlorides to CNs.

polymerization of EDA and CF. [17] XRD analysis in Fig. 2 shows a broad peak for CN-CF around 22° attributed to 002 reflection of hexagonal graphite, exemplifying a low graphitization. Raman spectra in Fig. S2 show two overlapping bands at 1350 cm^{-1} and 1570 cm^{-1} for all CNs. The D bond at 1350 cm^{-1} arises from disorder,[23] the G bond at 1570 cm^{-1} represents sp^2 bonded graphitic carbons.[24] Compared with CN-CT, the shifting of G peak towards lower wave numbers (from 1585 to 1568 cm^{-1}) and the broadening of G-peak in CN-CF are also indicators for the lower graphitization in carbon skeleton.[17]

Here, the structure of organic chlorides plays an important role in controlling the morphology of the resultant CNs. We choose three organic chlorides as carbon sources, that is carbon tetrachloride (CT), chloroform (CF) and tetrachloroethane (TE). We can see that one C atom is connected with 4 Cl atoms in CT, one C atom is connected with 3 Cl atoms and 1 H atom in CF, and two C atoms are connected with 4 Cl atoms and 2 H atom in TE (Scheme 1). In CNs' preparation, the mole of EDA is higher than that of organic chloride. The formation of CNs can be attributed to heat-treatment-induced polymerization of C-Cl and N-H, followed by the release of HCl. The C-Cl is active to N-H but C-H is inactive to N-H, resulting in that the final ploymer has more C-H bonds in CN-CF and CN-TE. The large amount of C-H bonds can be seemed as defect sites that could not patcitipate in polymerization and leads to low polymerization degree of the final ploymer. After carbonization, the ploymer with more C-H bonds exhibites more open pore structure (Scheme 2). Thus, CN-CF has higher BET area and pore size than CN-CT. Because
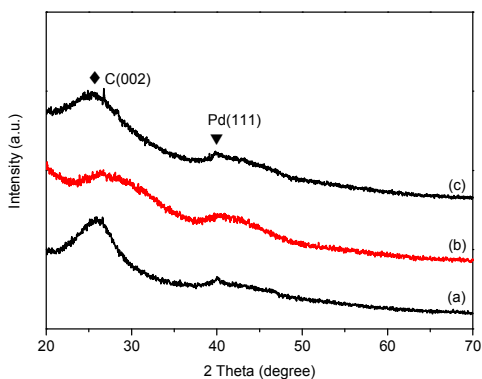
of the exsitence of C-C bond in TE, the corrosponding polymerization degree of final ploymer is higher than that of CF, and CN-CF is more porous than CN-TE. These deductions can be confirmed by N$_2$ asorption, TEM and SEM results. Therefore, the structure of organic chlorides determines the polymerization degree of ploymer, further predetermines the pore structure of the resulting CNs.

Elemental analysis shows that there is >12 wt % of nitrogen atoms in final CNs (Table S2). FTIR (Fig. S3) shows that the bands centered at 1207, 1630 and 3443 cm^{-1} are attributed to aromatic C–N stretching bonds, aromatic ring modes, and the stretching mode of the N-H groups in the aromatic ring, respectively.[17] High resolution XPS (Fig. s4a) demonstrates that the carbon atoms in CN-CF exist mainly in form of C-C/C=C (284.6 eV, 50.7 %) and aromatic C-N/C=N (285.7 eV, 44.1 %). The N envelope (Fig. S4b) demonstrates that the nitrogen atoms are mainly in form of N atoms bonded with the graphitic carbon atoms (398.2 eV, 46.3 %) and N atoms trigonally bonded to all sp^2 carbons (400.4 eV, 53.7 %).[25] As observed in elemental maps (Fig. S5b) and elemental analysis (Table S2) of CN-CF, the N content between surface and bulk is similar, and there is a good spatial correspondence of C and N elemental maps, indicating that N doping forms homogeneously over the entire carbon skeleton. Therefore, the carbon nitride
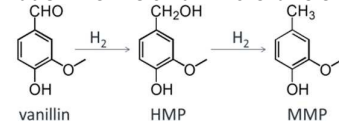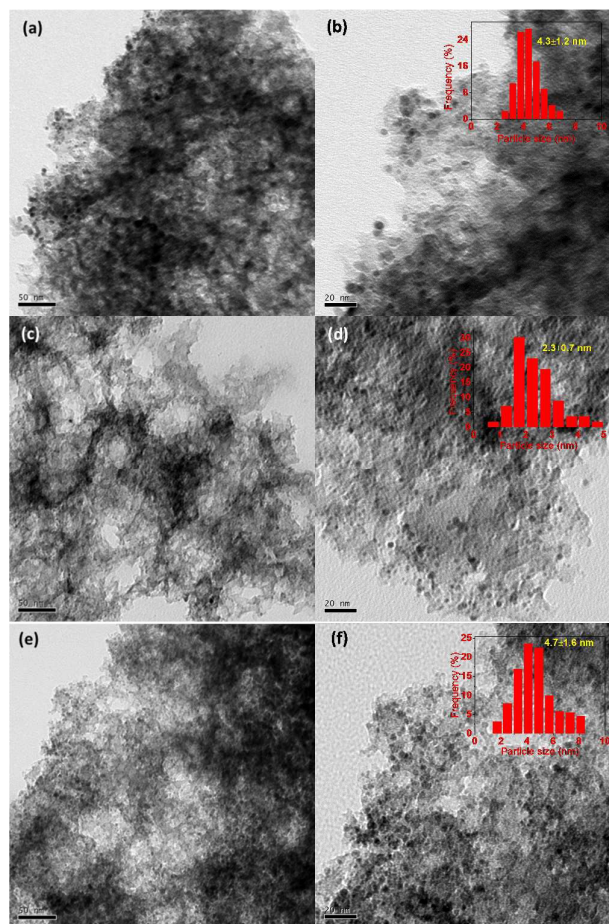

Fig. 2 XRD patterns of (a) Pd/CN-CT, (b) Pd/CN-CF and (c) Pd/CN-TE.

Fig. 3 TEM images of (a, b) Pd/CN-CT, (c, d) Pd/CN-CF and (e, f) Pd/CN-TE.

Table 2 The HDO of vanillin over different catalysts.[a]

Entry	Catalyst	T/^oC	t/h	Conversion / %	Selectivity / %		MMP yield / %
					HMP	MMP	
1	Pd/CN-CT	70	0.5	40	55	45	18.0
2	Pd/CN-CF	70	0.5	64	29	71	45.4
3	Pd/CN-TE	70	0.5	47	52	48	22.6
4	Pd/CN-CT	70	1	86	34	66	56.8
5	Pd/CN-CF	70	1	93	15	85	79.1
6	Pd/CN-TE	70	1	90	40	60	54.0
7	Pd/AC	70	1	78	53	47	36.7
8	Pd/CN-CF	50	7	99	1	99	98.0
9	Pd/CN-CF	90	1	99	2	98	97.0 (295.4 h^{-1})[e]
10[b]	Pd@CN$_{0.132}$	90	1	65	31	69	44.9 (157.0 h^{-1})[e]
11[c]	Pd/TiO$_2$@N-C	150	2	91	22	78	71 (29.5 h^{-1})[e]
12[d]	Ru/CNTs	100	3	95	87	13	12.4 (20.6 h^{-1})[e]

[a] Reaction conditions: vanillin (200 mg), catalyst (20 mg), S/C=306, H$_2$O (16 mL), 1 MPa H$_2$. [b] Reaction conditions: vanillin (1000 mg), S/C = 350, H$_2$O (80 mL), 1 MPa H$_2$; data taken from ref [9]. [c] Reaction conditions: vanillin (76 mg), 1.2 mol% of Pd, S/C=83, H$_2$O (10 mL), 1 MPa H$_2$; data taken from ref [21]. [d] Reaction conditions: vanillin (897 mg), 0.2 mol% of Ru, S/C=500, H$_2$O (40 mL), 1 MPa H$_2$; data taken from ref [22]. [e] Data in parentheses is the TOF value (moles of MMP produced per Pd mole per hour).

heterocycle of CN with rich nitrogen groups (especially for aromatic nitrogen) will provide a natural platform for the variability and immobilization of metal ions (Fig. S6), and the CN could be regarded as a well-defined nanoreactor for stabilizing and supporting Pd NPs.

The synthetic methodology of Pd NPs supported on CN involves metal coordination and chemical reduction. In brief, the Pd^{2+} is firstly introduced as complex ion of the N-rich CN backbone (Fig. S6), and the mixture is then mildly reduced by H$_2$ at pressurized atmosphere (Scheme 1). The XRD pattern (Fig. 2) of the as-prepared Pd/CNs shows a broad reflection at $2\vartheta = 40.0^o$ that assigned to (111) reflection of cubic (fcc) palladium lattice. But this characteristic peak becomes more broad and faint for CN-CF, indicating the presence of more dispersed Pd NPs on the surface of CN-CF. According to Scherrer's formula and the half-width of (111) peak (Table S1), the calculated sizes of Pd crystallites in Pd/CN-CT, Pd/CN-CF and Pd/CN-TE are 3.8, 2.1 and 4.5 nm, respectively.

The Pd dispersion on CNs has been further confirmed by TEM observations in Fig. 3. Pd NPs are not so even on the surface of CN-CT and CN-TE, in which the mean particle sizes are 4.3 and 4.7 nm, respectively. In contrast, the uniformly well-dispersed Pd NPs on very large surfaces of CN-CF can be observed (Fig. 3c and d), without any aggregation of NPs into large clusters, and the mean particle size is centered at 2.4 nm. Rich nitrogen in carbon skeleton is suitable for stabilizing highly dispersed Pd. As expected, Pd/CN-CF containes high percentage of Pd$^{\delta+}$ (40 %) as revealed by Pd 3d5/2 XPS peaks at 336.2 and 341.4 eV (Fig. S7), indicating the strong interaction between N and Pd.[26]

The HDO of vanillin in water over these CN supported Pd catalysts are carried out as a model reaction and these results are summarized in Table 2. Under 70 ^oC for 0.5 h, the yield of MMP reaches 18.0 %, 45.4 % and 22.6 % over Pd/CN-CT, Pd/CN-CF and Pd/CN-TE, respectively (entries 1-3). When the reaction time increases to 1 h, the catalytic activity of Pd/CN-CF still exceeds

those of Pd/CN-CT and Pd/CN-TE (entries 4-6), and shows better activity (93 %, entry 5) and MMP selectivity (85 %) than that of AC supported Pd catalyst (entry 7). Variation of reaction temperature has a considerable effect on vanillin conversion (entries 8 and 9). Conversion of 99 % is achieved with a MMP selectivity exceeding 99 % after a longer reaction time of 7 h at 50 ^oC (entry 8). The reaction is accelerated at higher temperature; for example, 99 % of conversion in 1 h is obtained at 90 ^oC with a high MMP selectivity of 98 % (entry 9, Fig. S8), in which the TOF is as high as 295.4 h^{-1}, comparable with most of the reported heterogeneous catalysts (Pd@CN$_{0.132}$: 157.0 h^{-1}; Pd/TiO$_2$@N-C: 29.5 h^{-1}; Ru/CNTs: 20.6 h^{-1}) for this reaction at same temperature or elevated temperatures.[9, 21, 22]

H$_2$ pressure has a large impact on catalytic activity (Fig. 4) and the observed conversion at 3.0 MPa (99 %) is more than 2.5 times higher than at 0.5 MPa. The selectivity towards MMP also increases
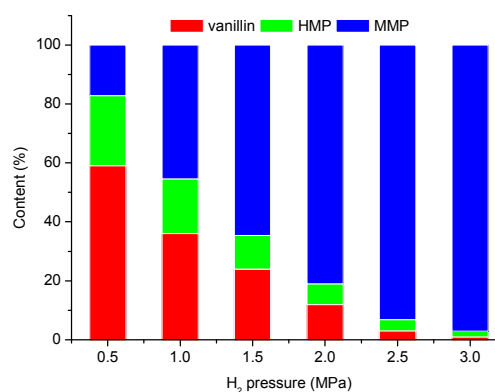

Fig. 4 H$_2$ pressure-activity profile for the selective hydrogenation of vanillin. Reaction conditions: vanillin (200 mg), Pd/CN-CF (20 mg), H$_2$O (16 mL), 70 ^oC, 0.5 h.
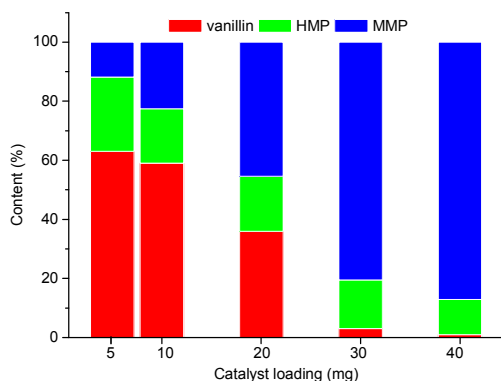
Fig. 5 Catalyst loading-activity profile for the selective hydrogenation of vanillin over Pd/CN-CF. Reaction conditions: vanillin (200 mg), H_2O (16 mL), 1 MPa H_2, 70 ^{o}C, 0.5 h.

considerably from 71 % to 98 % with increase of H_2 pressure from 0.5 to 3.0 MPa respectively. Upon increasing the catalyst loading (Fig. 5), vanillin is consumed gradually and converted almost completely with a loading of 40 mg. But higher catalyst loading at 40 mg could not afford full transformation of HMP to MMP. Therefore, the HDO of vanillin over Pd/CN-CF is more sensitive to H_2 pressure and reaction temperature in comparison to catalyst loading.

The better activity of Pd/CN-CF is attributed to its mesoporous structure and dispersed Pd NPs. The high dispersion of Pd NPs provides more active sites for catalytic HDO of reactants, while the highly mesoporous structure provides easily access of reactants to active sites. Meanwhile, the rich surface nitrogen can serve as Lewis basic sites to increase the hydrophilicity and basicity of CN (Fig. S9).[27] Zhou and co-workers synthesized a series of amphiphilic carbonaceous microspheres-supported Pd catalysts for the HDO of vanillin in both a pure aqueous phase and water–oil biphasic systems.[28] They found that the wettability of the catalyst could be
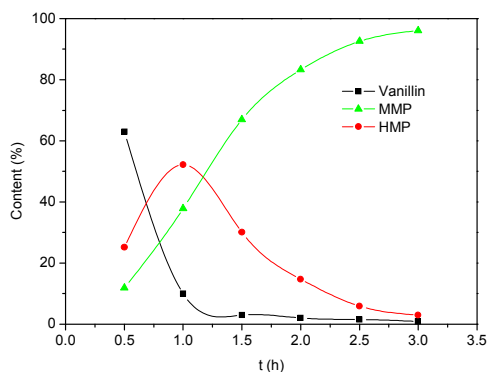

Fig. 6 Time-activity profile for the selective hydrogenation of vanillin. Reaction conditions: vanillin (200 mg), Pd/CN-CF (5 mg), H_2O (16 mL), 1 MPa H_2, 70 ^{o}C.

facilely tuned by adjusting the hydrothermal treatment temperature or by a post-treatment process in alkaline solution, and the more hydrophilic the catalyst, the more active it was for the HDO of vanillin in water. Here, the rich surface nitrogen could result in good hydrophilic property that benefits the dispersion of catalyst in water and wettability of the substrate on the support, hence accelerating the diffusion and transformation of substrates. The better MMP selectivity of Pd/CN-CF is attributed to mild catalytic condition and poor solubility of MMP in water (Fig. S10).[9] The poor solubility of newly generated MMP leads to its separation from the water phase and catalyst, depressing the further hydrogenolysis of MMP under this mild condition. The evolution of reactant and product with reaction time is performed over Pd/CN-CF catalyst (Fig. 6). It can be found that vanillin is easily hydrogenated to HMP in the first 1 h. Later, the hydrogenolysis of HMP proceeds rapidly due to its high concentration. After 3 h, almost all HMP has been converted to MMP *via* hydrogenolysis.

The Pd/CN-CF catalyst can be easily separated by extraction (Fig. S11) for several cycles without obvious lose of activity or MMP selectivity (Fig. S12). For example, the Pd/CN-CF catalyst in the sixth recycle has a TOF of 133 h^{-1}, which is still comparable with that to the fresh catalyst (139 h^{-1}). The ICP analysis of fresh and recovered catalysts reveals negligible Pd leaching (<0.05 ppm) in water solution and the observed catalysis is truly heterogeneous in nature (Fig. S13). The dispersion of Pd NPs in recovered Pd/CN-CF, based on the corresponding TEM image (Fig. S14), do not change significantly after six runs.

Conclusions

Mesoporous CN is prepared through polymerization by a hard-template method. The structure of organic chloride plays a crucial role in control of the degree of polymerization. The CN derived from CF exhibits a highly mesoporous backbone that owns superior talent for the control of Pd NPs and therefore endows CN-CF with dual roles (stabilization and support). The Pd NPs trapped in CN-CF affords outstanding performance in water phase for the selective HDO of vanillin at low pressure (<1 MPa) and temperature (<70 ^{o}C). This catalyst is reusable and affords much higher TOF (295.4 h^{-1}) than most reported catalysts.

Experimental

Materials

Fumed silica (SiO_2) with a specific surface area of 250 m^2/g was obtained from Degussa Co. (Germany). Ethylenediamine (EDA, AR), carbon tetrachloride (CT, AR), chloroform (CF, AR), tetrachloroethane (TE, AR), $PdCl_2$ (AR, Pd >59 %), vanillin (AR) and other chemicals (analytical grade) were purchased from Aladdin Chemicals and used without further purification.

Preparation of CN

In a typical process for CNs, 0.5 g fumed silica was dispersed into a mixed solution of ethylenediamine (EDA, 89.9 mmol) and carbon tetrachloride (CT, 78 mmol) under stirring. The above mixture was heated at 90 °C for 6 h and then dried in an oven for 12 h. The

template-carbon nitride polymer composite was subjected to 600 ^{o}C at a heating rate of 3 ^{o}C·min^{-1} under a flow of nitrogen and kept for 5 h. The carbonized material was treated with 5 wt. % hydrofluoric acid. The solid was recovered by filtration, washed with ethanol and dried at 100 ^{o}C. The resultant sample was denoted as CN-CT. For the synthesis of CN-CF and CN-TE, different organic chlorides (CF and TE) were used in place of CT under the same reaction conditions.

Preparation of CN supported Pd catalysts

One gram of CN was dispersed in DI water (50 mL), then added with 41.7 mg PdCl$_2$ (2.5 wt. %) while stirring. After 30 min, the reduction treatment was performed in a 100 mL Teflon-lined autoclave at 40 ^{o}C for 8 h under 2 MPa H$_2$. Then, the precipitate was recovered by filtration and washed thoroughly with DI water. The resulting Pd catalyst was dried in an oven at 80 ^{o}C overnight and named as Pd/CN. The real amount of loading Pd was detected *via* inductively coupled plasma-atomic emission spectroscopy (ICP, Plasma-Spec-II spectrometer) and summarized in Table S1.

Catalyst characterization

Powder X-ray diffraction (XRD) was performed on a Bruker D8A25 diffractometer with CuKα radiation (λ = 1.54184 Å) operating at 30 kV and 25 mA in the range of 10-80° 2θ. Fourier transform infrared (FTIR) spectra were analyzed on an OPUS Fourier Transform Infrared Spectrophotometer in the range of 400–4000 cm^{-1}. N$_2$ adsorption was carried out at -196 ^{o}C using an auto-adsorption analyzer (Micromeritics, TriStar II). X-ray photoelectron spectra (XPS) were recorded on a Perkin-Elmer PHI ESCA system. Scanning electron images (SEM) and surface compositions were collected on JEOL (JSM6700F)) with an accelerating voltage of 15 kV. Transmission electron microscope (TEM) images were obtained using an accelerating voltage of 200 kV on a JEOL-135 2010F Transmission Electron Microscope. Raman spectra were collected at room temperature from 100 to 4000 cm^{-1} with 514.5-nm argon ion laser (Rhenishaw Instruments, England).

Selective hydrogenation of vanillin

The hydrogenation reaction was carried out in a 50 mL stainless autoclave with a Teflon liner. In a typical procedure, 20 mg catalyst was dispersed in 16 mL DI water, and then added with 200 mg vanillin. The autoclave was sealed, purged and pressurized with hydrogen to 1.0 MPa, and then heated to 70 ^{o}C under magnetic stirring at a rate of 1000 rpm. After reaction, the autoclave was quickly cooled down within cold water. The organic compounds was extracted by ethyl acetate, the catalyst was recovered from aquouse phase by centrifugation and then washed several times with ethanol. The contents of products and substrate were analyzed by gas-chromatogram (GC, HP 5890, USA) with a 30 m capillary column (HP-5) using a flame ionization detector (FID). Interpolated calibration was employed for product quantification using standard solutions of vanillin, HMP and MMP. All the products were confirmed by GC–MS (Agilent 6890).

Acknowledgements

Notes and references

1. R. Sharma and N. Bakhshi, *Energy & Fuels*, 1993, **7**, 306-314.
2. A. Singh, D. Pant, N. Korres, A. Nizami, S. Prasad and J. Murphy, *Bioresour. Technol.*, 2010, **101**, 5003-5012.
3. F. H. Mahfud, S. Bussemaker, B. J. Kooi, G. H. Ten Brink and H. J. Heeres, *J. Mol. Catal. A,* 2007, **277**, 127-136.
4. S. Crossley, J. Faria, M. Shen and D. Resasco, *Science*, 2010, **327**, 68-72.
5. B. Puértolas, T. C. Keller, S. Mitchell and J. Pérez-Ramírez, *Appl. Catal. B*, 2016, **184**, 77-86.
6. T. Vispute and G. Huber, *Green Chem.*, 2009, **11**, 1433-1445.
7. J. Bredenberg, M. Huuska, J. Raty and M. Korpio, *J. Catal.*, 1982, **77**, 242-247.
8. Y. Wang, T. He, K. Liu, J. Wu and Y. Fang, *Bioresour. Technol.*, 2012, **108**, 280-284.
9. X. Xu, Y. Li, Y. Gong, P. Zhang, H. Li and Y. Wang, *J. Am. Chem. Soc.*, 2012, **134**, 16987-16990.
10. Y.-C. Lin, C.-L. Li, H.-P. Wan, H.-T. Lee and C.-F. Liu, *Energy & Fuels*, 2011, **25**, 890-896.
11. J. Sun, A. Karim, H. Zhang, L. Kovarik, X. Li, A. Hensley, J. Mcewen and Y. Wang, *J. Catal.*, 2013, **306**, 47-57.
12. T. Pham, L. Lobban, D. Resasco and R. Mallinson, *J. Catal.*, 2009, **266**, 9-14.
13. A. Centeno, B. Delmon and E. Laurent, *J. Catal.*, 1995, **154**, 288-298.
14. M. Ferrari, B. Delmon and P. Grange, *Carbon*, 2002, **40**, 497-511.
15. P. Gallezot, S. Chaumet, A. Perrard and P. Isnard, *J. Catal.*, 1997, **168**, 104-109.
16. Y. Wang, X. Wang and M. Antonietti, *Angew. Chem. Int. Ed.*, 2012, **51**, 68-89.
17. A. Vinu, *Adv. Funct. Mater.*, 2008, **18**, 816-827.
18. M. Groenewolt and M. Antonietti, *Adv. Mater.*, 2005, **17**, 1789-1792.
19. Y. Liang, Y. Li, H. Wang, J. Zhou, J. Wang, T. Regier and H. Dai, *Nature mater.*, 2011, **10**, 780.
20. X. Xie, J. Long, J. Xu, L. Chen, Y. Wang, Z. Zhang, and X. Wang, *RSC Adv.*, 2012, **2**, 12438-12446.
21. L. Wang, B. Zhang, X. Meng, D. S. Su and F.-S. Xiao, *ChemSusChem*, 2014, **7**, 1537-1541.
22. X. Yang, Y. Liang, Y. Cheng, W. Song, X. Wang, Z. Wang and J. Qiu, *Catal. Commun.*, 2014, **47**, 28-31.
23. H. Wang, X. Xiang and F. Li, *J. Mater. Chem.*, 2010, **20**, 3944-3952.
24. V. Chandra, J. Park, Y. Chun, J. W. Lee, I.-C. Hwang and K. S. Kim, *ACS Nano*, 2010, **4**, 3979-3986.
25. A. Thomas, A. Fischer, F. Goettmann, M. Antonietti, J.-O. Müller, R. Schlögl and J. M. Carlsson, *J. Mater. Chem.*, 2008, **18**, 4893.
26. R. Arrigo, M. E. Schuster, Z. Xie, Y. Yi, G. Wowsnick, L. L. Sun, K. E. Hermann, M. Friedrich, P. Kast, M. Hävecker, A. Knop-Gericke and R. Schlögl, *ACS Catal.*, 2015, **5**, 2740-2753.
27. E. Haque, J. W. Jun, S. N. Talapaneni, A. Vinu and S. H. Jhung, *J. Mater. Chem.*, 2010, **20**, 10801-10807.
28. Z. Zhu, H. Tan, J. Wang, S. Yu and K. Zhou, *Green Chem.*, 2014, **16**, 2636-2643.

Graphic abstract
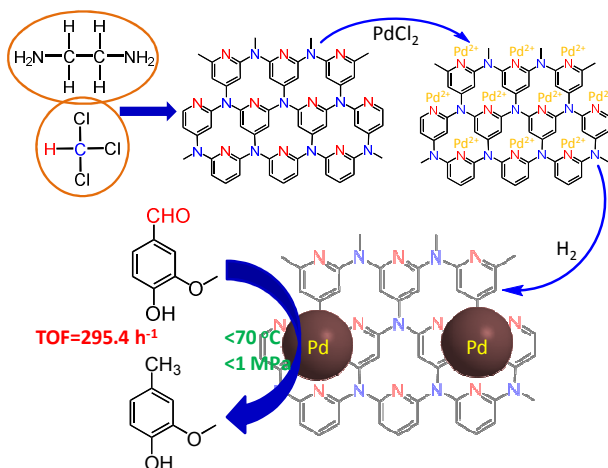
     Mesoporous carbon nitride (CN) is prepared *via* polymerization between ethylenediamine and chloroform. This basic network with open channels renders homogeneously dispersed Pd coordinated in the mesoporous carbonaceous framework and creates a highly active and stable Pd/CN catalyst for the selective HDO of vanillin at low H_2 pressure (<1.0 MPa) and temperature (<70 ^{o}C). The Pd/CN is reusable and the best TOF of all Pd atoms reaches 295.4 h^{-1}.